El Mustafa Ouaaka[1], Said Kassou[2], Mahmoud Ettakni[1], Salaheddine Sayouri[3], Ahmed Khmou[1], El Mostafa Khechoubi[1]

Electronic Structure and Thermoelectric Properties of Hybrid Organic-Inorganic Perovskites [NH₃-(CH₂)₃-COOH]₂CdCl₄

[1]*Department of Physics, Faculty of Science, Materials and Renewable Energies team, LP2MS Laboratory, University Moulay Ismail, Zitoune, Meknes, Morocco, khechoubi@umi.ac.ma*
[2]*Department of Physics, R&D Center for Membrane Technology and Center for Nanotechnology, Chung Yuan Christian University, Taoyuan, Taiwan*
[3]*LPTA, Faculty of Sciences-DM, USMBA, Fez-Atlas, Morocco*

In this work, we conducted the first principle calculation of electronic structure and transport properties of [NH₃-(CH₂)₃-COOH]₂CdCl₄ (Acid-Cd). The generalized gradient approximation is used in structural optimization and electronic structure. The theoretical band gap value found is in good agreement with experimental. Electronic thermal conductivity, electrical conductivity, Seebeck coefficient (S) and figure of merit (ZT) have been calculated using semi-local Boltzmann theory to predict the thermoelectric characteristic of the studied materials.

Keywords: hybrid organic inorganic; band structure; density of states; gap energy; electrical conductivity; Seebeck coefficient; figure of merit.

Introduction

Thermoelectric materials can convert the thermal energy to electricity via Seebeck effect, which was discovered by Seebeck [1]. The Seebeck coefficient was obtained from the ratio of the applied temperature difference and the voltage generated.

$$S = \frac{\Delta V}{\Delta T}$$

The dimensionless figure of merit ZT [2] can be assessed the performance of thermoelectric materials.

$$ZT = \frac{S^2 \sigma T}{\kappa}$$

Where σ and k denote the electrical and thermal conductivities, where S represents the Seebeck coefficient at defined temperature T.

The current low thermoelectric conversion efficiency has restricted wider applications of the thermoelectric device. Increasing interest is to increase entire thermoelectric conversion efficiency. Generally, inorganic thermoelectric materials [3-8] have higher figure-of-merit (*ZT*) than that of organic thermoelectric materials [9], but their rigid and brittle properties symbolize those inorganic thermoelectric materials need substrates to make them flexibility. By contrast, organic thermoelectric materials have properties containing low thermal conductivity (κ), excellent flexibility, and low cost [10]. Other shortcomings for developed inorganic thermoelectric materials are their toxic nature and high cost [11].

Many studies have focused on combine the high thermoelectric performance of inorganic material and high flexibility of organic materials in one bulk [12, 13].

Organic-inorganic hybrid materials have attracted more interest due to their interesting properties such as optical [14, 15], ferroelectric [16, 17], electronic [18, 19] and magnetic [20, 21]. Their structure is made of alternating layers between inorganic and organic parts and

they possess new properties intermediate between those of the two constituent parts [22, 23]. Inorganic units can be self-organized into low dimensional crystals, where they form three (3D), two (2D), one (1D), and zero (0D) dimensional networks according to the organic cations.

We note that the $CH_3NH_3PbI_3$ wich is the most using organic inorganic materials has a very low thermal conductivity of pseudo cubic phase [24]. A Seebeck coefficient of about 1600µV/K has been found for $CH_3NH_3PbI_3$ and $NH_2CHNH_2PbI_3$ while for $CH_3NH_3SnI_3$ and $NH_2CHNH_2SnI_3$ is about 800 µV/K. these results are higher than that of p-type semiconductor Bi_2Te_3 [25].

In this work, we have investigated electronic and thermoelectric properties of $[NH_3-(CH_2)_3-COOH]_2CdCl_4$ namely acid-Cd. We use DFT calculation to survey the partial density of states and electronic structure. The calculated electronic structure is introduced in Boltzrap code to evaluate thermal conductivity and electrical conductivity, Seebeck coefficient (S) and figure of merit (ZT).

I. Computation details

The electronic properties of acid-Cd perovskites were studied using DFT calculations implemented in ABINIT code [26, 27], with generalized gradient approximation (GGA) in the Perdew-Burke-Ernzerhof functional [28], using the plane wave pseudo potential formalism [29, 30]. A kinetic energy cutoff 500 eV was taken to perform the geometry optimization of acid-Cd. The Monkhorst Pack Mesh scheme [31] k-points grid sampling was set at 6x6x3 to perform the irreducible Brillouin zone integrations of acid-Cd. The thermoelectric properties were calculated using BoltzTraP code [32]. We use a starting point the crystal data of $[NH_3-(CH_2)_3-COOH]_2CdCl_4$ reported in the literature [33].

II. Results and discussions

The organic-inorganic acid-Cd compound perovskites has a monoclinic structure with space group $_1 P_{2_1}$ and lattice parameters a = 7.409(1) Å, b = 7.490(1) Å, c = 15.298(2) Å, β = 100.084(2)° and Z = 2 [33]. Fig. 1 shows the crystal structure of acid-Cd.
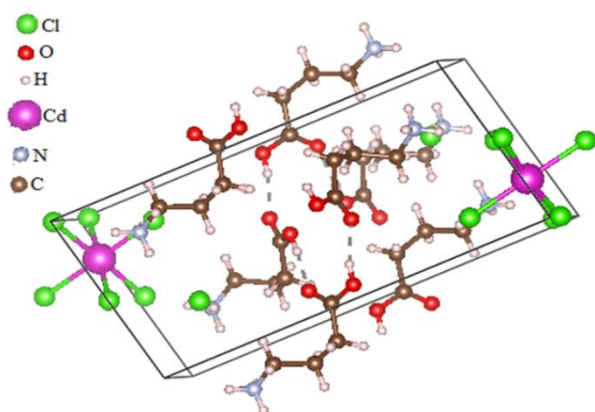

Fig. 1. Crystal structure of acid-Cd [33].

The cohesion of crystal packing is established by hydrogen bonds N-H … Cl between organic and inorganic components and by Van Der Waals interaction between cation-cation, anion-anion, and cation-anion.

2.1. Electronic properties

The electronic properties of acid-Cd including density of states and band structures were calculated after the optimization of the lattice parameters. Figure 2 shows the calculated electronic band structures of acid-Cd.
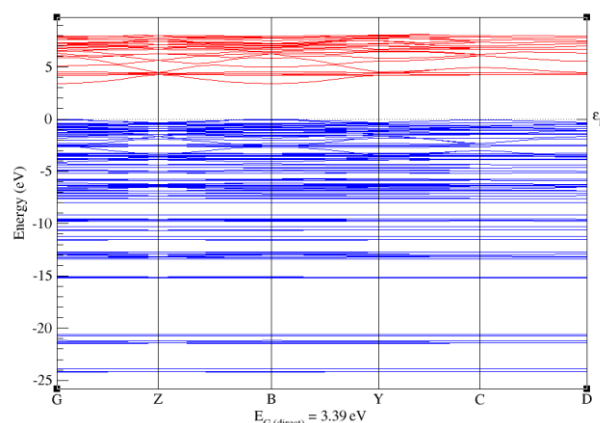

Fig. 2. Electronic band structures of acid-Cd.

It is clearly seen that this compound exhibits a direct band gap located at G point. the band gap of acid-Cd is found to be 3.39 eV, this result is in good agreement with that experiment [34]. The partial density of states (PDOSs) was calculated to understand the chemical bonding of each component. In the acid-Cd compound (Fig. 3), the range energy -20 to -10 eV is the feature of the mixed contribution between Np, C(s, p), Hs and Cls orbitals of nitrogen, carbon, hydrogen and chlorine respectively. This result due to the contribution organic electronic density part $NH_3-(CH_2)_3-COOH$ and hydrogen band Cl…H-N. The range energy from -9 to 0 eV wich constitutes the maximum of the valence band (MVB) is composed by mixed states Cd_d, Cl_p, C_p and O_p orbitals of cadmium, chlorine, carbone and oxygen respectively. This result due to the significance contribution of inorganic moieties $CdCl_4$ and hydrogen band C-O…H in the (MVB).

The minimum of conduction band (MCB) consists of atomic orbitals Op, Clp, and Cds. Due to the contribution electronic density of inorganic part $CdCl_4$ and hydrogen band C-O…H. this result show yhat the charge transfer in acid-Cd is established by both organic and inorganic moieties. Furhermore, the theoretical gap energies values calculated of acid-Cd is shown in Table 1. It is in reasonable agreement with experimental and theoretical values.

Table 1

Experimental and theoretical gap energies values of acid-Cd.

Experimental E_g (eV)	Theoretical E_g (eV)
3.65 [34] 3.28 [35] 2.19 [36]	3.39 our work(acid-Cd) 2.2 [36]

2.2. Thermoelectric properties

The thermoelectric properties of acid-Cd compound were investigated using the semi local Boltzmann theory incorporated in the BoltzTraP code. The performance of these properties for a material is described by a dimensionless parameter figure of merit (ZT) given by:

$$ZT = \frac{S^2 \sigma T}{k},\qquad(1)$$

where σ and κ denote the electrical and thermal conductivities, where S represents the Seebeck coefficient at a temperature T. On the other hand, the value of the thermal conductivity should be lower, however, the electrical conductivity and Seebeck coefficient should be higher for the best figure of merit (ZT).

Figure 4 shows the calculation of electronic thermal and electrical conductivities, Seebeck coefficient (S) and figure of merit (ZT) in the temperature range from 100 to 800 K. The electrical and electronic thermal conductivities shown in Figs. 4, (a) and (b) increase with increasing the temperature, and reach their maximum value of 4.10^{19} (Ω^{-1} m^{-1} s^-) and 9.10^{14} (WK^{-1} m^{-1} s^{-1}) respectively at 800 K. Fig. 4(c) illustrates the temperature dependence of the Seebeck coefficient. One can note that
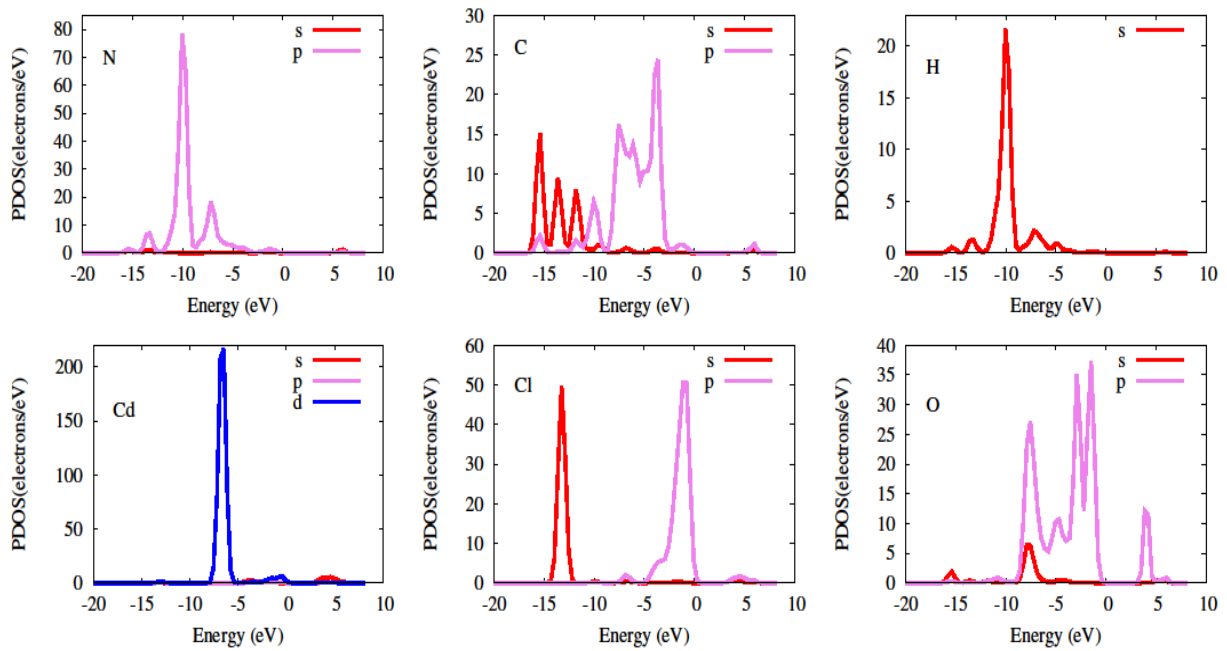

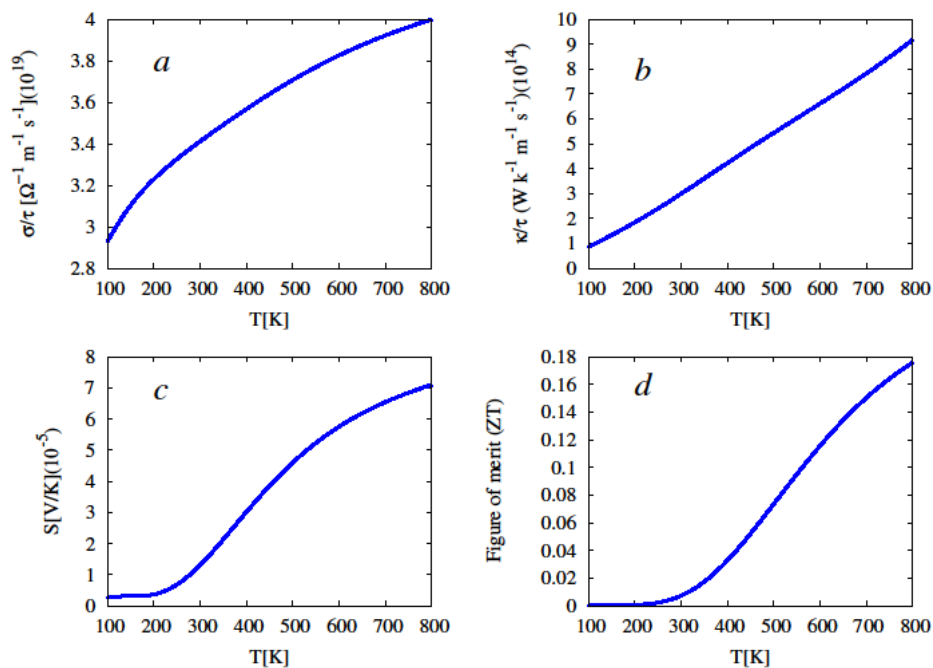**Fig. 3.** Partial density of states of acid-Cd.

Fig. 4.(a) Electrical conductivity, (b) thermal conductivity, (c) Seebeck coefficient and (d) figure of merit vs temperature of acid-Cd.

this coefficient is almost constant in the range of temperature 100 - 200 K. at 250 K (inflection point) the seebeck coefficient increases almost linearly and reaches its maximum value around $7 \cdot 10^{-5}$ V/K at 800 K. Furthermore, the figure of merit (ZT) displayed in Fig. 4,d exhibits almost the same behavior as in Fig. 4,c, and shows a sharp increase upon the increase of the temperature then reaches its maximum value around 0.18 at 800 K. Fig. 5 show the seebeack, electrical conductivity and thermal conductivity as a functional of chemical potential (µ) at various temperatures ranging from 300 to 600 K.
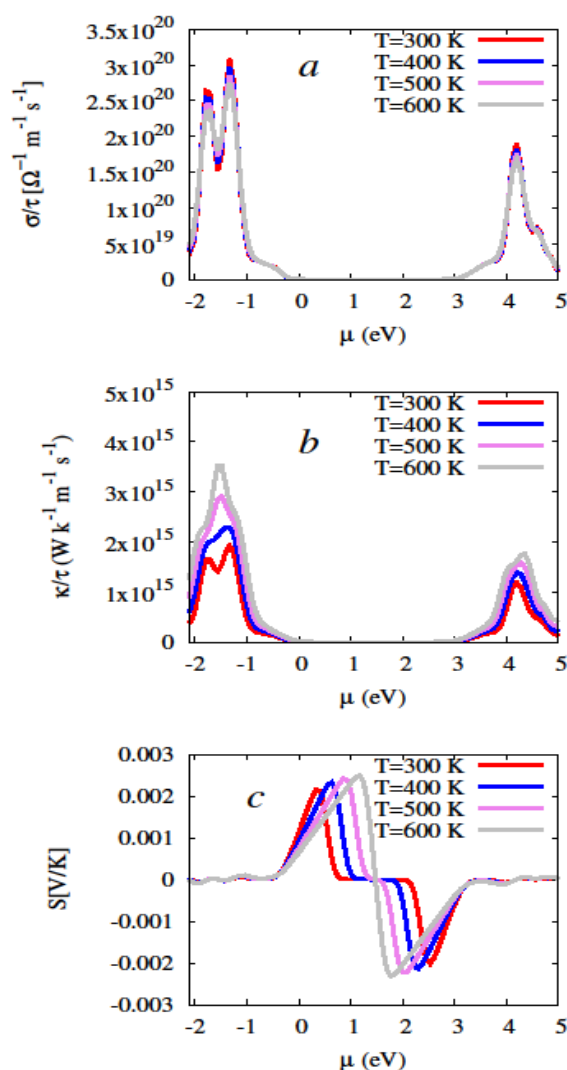

Fig. 5 (a) Electrical conductivity, (b) thermal conductivity, (c) Seebeck coefficient vs chemical potential µ of acid-Cd.

Fig. 5 (a) shows the result of the electrical conductivity of acid-Cd for different temperatures (300, 400, 500 and 600 K) as a function of the chemical potential from -2 to 5 eV. We see that electrical conductivity is almost independent of temperature with a maximum value (µ= -1.25 eV) is $3.12 \cdot 10^{20}$ $(\Omega ms)^{-1}$ at

300 K for p-type and decreases to $2.75 \cdot 10^{20}$ $(\Omega ms)^{-1}$ at 600 K. The thermal conductivity versus chemical potential is plotted in Fig. 5,(b). We can note that the electronic thermal conductivity (κ/τ) as a function of chemical potential for different temperature present the same shape that for σ. For µ= -1.25 eV the k increase from $2 \cdot 10^{15}$ W/mKs (at 300K) to $3.55 \cdot 10^{15}$ W/mKs (at 600 K), wich due to the increasing the carrier concentration.

Fig. 5(c) depicts the Seebeck coefficient versus chemical potential. Usually, the value of the Seebeck coefficient should be larger than 200 µV/K in the efficient thermoelectric materials [37]. We found that our calculated values for the Seebeck coefficient (Fig. 5(c)) are larger than the Bi_2Te_3 and Bi_2Se_3 systems [38]. Generally, the seebeck coefficient (S) is sensitive to chemical potential and temperature. The very high seebeck coefficient of acid-Cd originates from the mixed density of states (DOS) Cd_d, Cl_p, O_p and C_p atomic orbitals of valence bands. From the Fig. 5(c), we can note that the maximum of the seebeck coefficient increases as function the temperature T. This phenomenon is due to the intrinsic bipolar effect of the material [37]. The value of S equal to zero in the chemical potential range from 0.70 eV to 2.1 eV. The range of chemical potential for S = 0 becomes narrower with the increasing of temperature for the major raison of electronic excitation become easy with increasing of temperature.

Conclusion

In this work, we have studied the electronic and thermoelectric properties using DFT method. Our results indicate that the compound acid-Cd exhibit a direct and large band gap Eg of 3.39 eV. The thermoelectric properties of acid-Cd, including the thermal and electrical conductivities, Seebeck coefficient, and figure of merit were calculated as a function of temperature and chemical potential. A figure of merit (ZT) 0.18 and Seebeck coefficient $7 \cdot 10^{-5}$ VK^{-1} parameter has found at 800 K.

Elmustafa Ouaaka - PhD, Senior Researcher;
Said Kassou - PhD, Researcher;
Mahmoud Ettakni - Professor, Ph.D, Department of Physics;
Salaheddine Sayouri - Emeritus Professor, Ph.D, Department of Physics;
Ahmed Khmou - Emeritus Professor, Ph.D, Department of Physics;
El Mostafa Khechoubi - Professor, Ph.D., Head of Materials and Renewable Energies team, Department of Physics.

[1]   T.J. Seebeck, Proc. Prussian Acad. Sci. 265 (1822).

[2]   J. Mao, H. Zhu, Z. Ding, Z. Liu, Gamage. G.A., Chen. G., Ren Z., Science 365(6452), 495 (2019); https://doi.org/10.1126/science.aax7792.

[3]   Y. Pei, X. Shi., A. LaLonde., H. Wang., L. Chen, G.J. Snyder, Nature 473(7345), 66 (2011); https://doi.org/10.1038/nature09996.

[4]   W. Liu, X. Shi, R. Moshwan, M. Hong, L. Yang, Z.G. Chen, J. Zou, Sustainable Materials and Technologies 17, p.e00076 (2018); https://doi.org/10.1016/j.susmat.2018.e00076.

[5]   M. Hong, K. Zheng, W. Lyv, M. Li, X. Qu., Q. Sun., S. Xu., J. Zou, Z.G. Chen,Energy & Environmental Science 13(6), 1856 (2020); https://doi.org/10.1039/D0EE01004A.

[6]   X. Shi, Z.G. Chen, W. Liu, L. Yang, M. Hong, R. Moshwan., L. Huang, J. Zou, Energy Storage Materials 10, 130 (2018); https://doi.org/10.1016/j.ensm.2017.08.014.

[7]   A. Suwardi, J. Cao, Y. Zhao, J. Wu, S.W. Chien., X.Y. Tan, L. Hu, X. Wang., W. Wang, D. Li, Y. Yin, Materials Today Physics 14, 100239 (2020); https://doi.org/10.1016/j.mtphys.2020.100239.

[8]   M. Hong, Z.G. Chen, J. Zou, Chinese Physics B 27(4), 048403 (2018); https://doi.org/10.1088/1674-1056/27/4/048403.

[9]   Y. Zhang, Park. S.J. Polymers, 11(5), 909 (2019); https://doi.org/10.3390/polym11050909.

[10] M. Bharti, A. Singh, S. Samanta, D.K. Aswal, Progress in Materials Science 93, 270 (2018); https://doi.org/10.1016/j.pmatsci.2017.09.004.

[11] Y. Du., J. Xu, B. Paul, P. Eklund, Applied Materials Today 12, 366 (2018); https://doi.org/10.1016/j.apmt.2018.07.004.

[12] X.L. Shi, J. Zou, Z.G. Chen, Chemical Reviews 120(15), 7399 (2020); https://doi.org/10.1021/acs.chemrev.0c00026.

[13] L. Zhang, S. Lin, T. Hua, B. Huang, S. Liu, X. Tao, Advanced Energy Materials 8(5), 1700524 (2018); https://doi.org/10.1002/aenm.201700524.

[14] K.I. Sakai, M. Takemura, Y. Kawabe, Journal of luminescence 130(12), 2505 (2010); https://doi.org/10.1016/j.jlumin.2010.08.026.

[15] K. Pradeesh, G.S. Yadav, M. Singh, G.V. Prakash, Materials Chemistry and Physics 124(1), 44 (2010) https://doi.org/10.1016/j.matchemphys.2010.07.037.

[16] M. Bujak, J. Zaleski, Crystal Engineering 4(2-3), 241 (2001); https://doi.org/10.1016/S1463-0184(01)00018-1.

[17] K. Karoui, A.B. Rhaiem, K. Guidara, Physica B: Condensed Matter. 407(3), 489 (2012); https://doi.org/10.1016/j.physb.2011.11.021.

[18] M. Zdanowska-Frączek, K. Hołderna-Natkaniec, Z.J. Frączek, R. Jakubas, Solid State Ionics 180(1), 9 (2009); https://doi.org/10.1016/j.ssi.2008.10.018.

[19] I. Chaabane, F. Hlel, K. Guidara, Journal of alloys and compounds 461(1-2), 495 (2008); https://doi.org/10.1016/j.jallcom.2007.07.031.

[20] A.K. Vishwakarma, P.S. Ghalsasi, A. Navamoney, Y. Lan, A.K. Powell, Polyhedron 30(9), 1565 (2011); https://doi.org/10.1016/j.poly.2011.03.025.

[21] C. Aruta, F. Licci, A. Zappettini, F. Bolzoni, F. Rastelli, P. Ferro, T. Besagni, Applied Physics A 81(5), 963 (2005); https://doi.org/10.1007/s00339-004-3102-3.

[22] D.B. Mitzi, K. Chondroudis, C.R. Kagan, IBM journal of research and development 45(1), 29 (2001); https://doi.org/10.1147/rd.451.0029.

[23] D.B. Mitzi, Journal of the Chemical Society, Dalton Transactions (1), 1 (2001); https://doi.org/10.1039/B007070J.

[24] X. Qian, X. Gu, R. Yang, Applied Physics Letters 108(6), 063902 (2016); https://doi.org/10.1063/1.4941921.

[25] C. Lee, J. Hong, A. Stroppa, M.H. Whangbo, J.H. Shim, Rsc Advances 5(96), 78701 (2015); https://doi.org/10.1039/C5RA12536G.

[26] X. Gonze, B. Amadon, P.M. Anglade, J.M. Beuken, F. Bottin, P. Boulanger, F. Bruneval, D. Caliste, R. Caracas, M. Côté, T. Deutsch, Computer Physics Communications 180(12), 2582 (2009); https://doi.org/10.1016/j.cpc.2009.07.007.

[27] X. Gonze, J.M. Beuken, R. Caracas, F. Detraux, M. Fuchs, G.M. Rignanese, L. Sindic, M. Verstraete, G. Zerah. F. Jollet, M. Torrent, Computational Materials Science 25(3), 478 (2002); https://doi.org/10.1016/S0927-0256(02)00325-7.

[28] J.P. Perdew, K. Burke, M. Ernzerhof, Physical review letters 77(18), 3865 (1996); https://doi.org/10.1103/PhysRevLett.77.3865.

[29] P. Hohenberg, W. Kohn, Physical review 136(3B), B864 (1964); https://doi.org/10.1103/PhysRev.136.B864.

[30] W. Kohn, L.J. Sham, Physical review 140(4A), A1133 (1965); https://doi.org/10.1103/PhysRev.140.A1133.

[31] H.J. Monkhorst, J.D. Pack, Physical review B 13(12), 5188 (1976); https://doi.org/10.1103/PhysRevB.13.5188.

[32] G.K. Madsen, D.J. Singh, Computer Physics Communications 175(1), 67 (2006); https://doi.org/10.1016/j.cpc.2006.03.007.

[33] M. Ettakni, A. Kaiba, J. Aazza, F. Haiki and M. Khechoubi, Journal of Asian Scientific Research 5(9), 473 (2015); https://doi.org/10.18488/journal.2/2015.5.9/2.9.473.481.

[34] M.B. AlShammari, A. Kaiba, P. Guionneau, M.H. Geesi, T. Aljohani, Y. Riadi, Chemical Physics Letters 702, 8 (2018); https://doi.org/10.1016/j.cplett.2018.04.051.
[35] K. Karoui, Journal of Molecular Structure 1203, 127430 (2020); https://doi.org/10.1016/j.molstruc.2019.127430.
[36] Q. Wang, M. Ma, K. Cui, Y. Li, X. Wu, Journal of Alloys and Compounds 854, 157187 (2021); https://doi.org/10.1016/j.jallcom.2020.157187.
[37] J. Sun, D.J. Singh, Physical Review Applied 5(2), 024006 (2016); https://doi.org/10.1103/PhysRevApplied.5.024006.
[38] X. Luo, M.B. Sullivan, S.Y. Quek, Physical Review B 86(18), 184111 (2012); https://doi.org/10.1103/PhysRevB.86.184111.

Ел М. Оуака[1], С. Кассоу[2], М.Еттакні[1], С. Сайоурі[3], А. Хмоу[1], Ел М. Хечоубі[1]

Електронна структура та термоелектричні властивості гібридних органічно-неорганічних перовкситів [NH₃-(CH₂)₃-COOH]₂CdCl₄

[1]*Кафедра фізики, Факультет наук, матеріалів та відновлюваних джерел енергії, Університет Мулай Ісмаїла, Зітун, Мекнес, Марокко*
[2]*Кафедра фізики, науково-дослідний центр мембранних технологій та центр нанотехнологій Християнського університету Чунг Юань, Таоюань, Тайвань*
[3]*LPTA, Факультет наук-DM, USMBA, Фес-Атлас, Марокко*

У роботі виконано першопринципний розрахунок електронної структури та транспортних властивостей структри [NH₃-(CH₂)₃-COOH]₂CdCl₄ (Acid-Cd). Для оптимізації структури та аналізу електронної структури використано узагальнену градієнтну апроксимацію. Знайдено теоретичне значення ширини забороненої зони, яке добре узгоджується з експериментом. Електронна теплопровідність, електропровідність, коефіцієнт Зеєбека (S) і добротність (ZT) розраховано із використанням напівлокальної теорії Больцмана для прогнозування термоелектричних характеристик досліджуваних матеріалів.

Ключові слова: гібридні органічно-неорганічні структури; зонна структура; густина станів; енергія забороненої зони; електропровідність; коефіцієнт Зеєбека; термоелеткрична добротність.